Stress-strain state of a glass panel with adhesive point fixings

E.N. Gerasimova[a*], A.V. Galyamichev[a], M.K. Mikhaylova[b], S. Dogru[c]
[a] *Peter the Great St. Petersburg Polytechnic University, St. Petersburg, Russia*
[b] *NIUPTS «Mezhregional'nyy institut okonnykh i fasadnykh konstruktsiy», St. Petersburg, Russia*
[c] *Istanbul Okan University, Istanbul, Turkey*
* E–mail: katyageras17@gmail.com

Abstract. The article is devoted to the study on the bearing capacity of the glazing with adhesive point fixings. This article provides evaluation of such factors as applied load, edge distance, panel thickness and number of point fixtures and their influence on stress-strain state of a glazing panel. Calculation of the panels under various conditions was performed by means of Finite Element Method (FEM). Results of the calculation show dependencies between considered factors and stress-strain state of a panel and present an overview of the on the possibilities of usage of such structures in accordance with Ultimate Limit State and Serviceability Limit State.

1. Introduction

Nowadays facade glazing is the most widespread type of enclosing structure used in public buildings and facilities. Structural façade, the particular type of translucent facade structures, allows to avoid presence of visible elements of the framework outside the building. It also increases the amount of daylight coming through enclosing structure and creates uniform and smooth surface of the façade.

A.A. Magay and N.V. Dubynin in the article [1] classify translucent facades by architectural and structural criteria. Based on second feature, the authors distinguish mullion-transom, frame, spider, structural, semi-structural, ventilated and panel types of facades. They also analyze the structural solutions and practical application of these options.

The main research purpose of [2] is the classification of a structural glazing.

Drass M., Schneider J., Odenbreit C., Kolling S. in [3–7] describe the main characteristics of Transparent Silicone Structural Adhesive (TSSA) and investigate the new nano-model of this material.

Pascual C., Montali J., Overend M. in article "Adhesively-bonded GFRP-glass sandwich components for structurally efficient glazing applications" show the results of the torsion and shear tests performed on silicone samples and introduce new analytic models for determination of deflections and stresses in the structure fixed by silicone adhesives [8].

Sitte S., Brasseur M.J., Carbary L.D., Wolf A.T. in their research "Preliminary Evaluation of the Mechanical Properties and Durability of Transparent Structural Silicone Adhesive (TSSA) for Point Fixing in Glazing" perform a preliminary evaluation of TSSA and present information regarding its durability and physical properties. Authors in [14–20] consider adhesive point fixation by means of TSSA and subject samples to various tests with following analysis of the results.

Articles [10, 11] are dedicated to the consideration of wind loads which act on façade structures. Authors in [12, 13] investigate problems which arise in curtain wall during its expoitation.

The object of study presented in this research is a stress-strain state of glass façade panels which have point fixation to bearing structure (routel of a spider fitting in a structural glazing)

Nowadays there is neither normative documentation for design of a structural glazing nor for evaluation of an adhesive point fixation. In foreign references researchers analyze the material itself, but without further investigation of its performance within the structure.

The main purpose of this research work was a determination of the factors which directly influence design of a curtain wall with adhesive point fixation.

Authors analyzed the results of a panel calculation while changing following parameters:

- Number of point fixtures;
- Thickness of a façade panel;
- Value of fixture edge distance.

Dow Corning is at the moment a major manufacturer of silicone adhesives. The technical guideline of this company [22] provides the percentage distribution of applied load to each fixture. Present article also verifies the information provided by the manufacturer.

The calculation was carried out on example of the most common panels with the dimensions 600×1200 mm, 1100×2100 mm and 2100×4200 mm, where first value is a width and second is a height of a panel. These sizes were adopted in order to investigate the panels of different dimensions but with the same side ratio.

Figure 1. Silicone film of a thickness of 1 mm [21].

Figure 2. View of a fixture from outside [21].

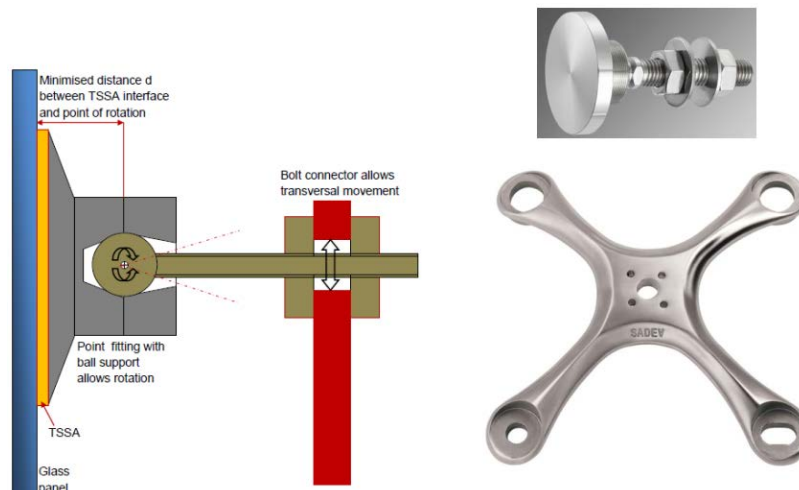**Figure 3. View of a fixture from inside [21].**

Figure 4. Fixture detail [22].

2. Methods

2.1. Physical model

Flat toughened glass with following characteristics according to Russian State Standard GOST 30698-2014 "Tempered glass" was used for the analysis:

- Density:

$$\rho = 2500 \text{ km/m}^3;$$

- Young's modulus:

$$E = 70\,000 \text{ N/mm}^2;$$

Герасимова Е.Н., Галямичев А.В., Михайлова М.К., Догру С.

- Poisson's ratio:

$$\upsilon = 0.2$$

- Considered thickness of a panel:

$$t = 8, 10, 12, 14, 16, 18 \text{ mm};$$

- Considered number of point fixtures:

$$n = 4, 6, 8.$$

2.2. Boundary conditions

One point on the top of a panel was fixed in *x, y* and *z* directions for compensation of temperature stresses, the second one was fixed in y and z directions, the others were fixed in y direction only.
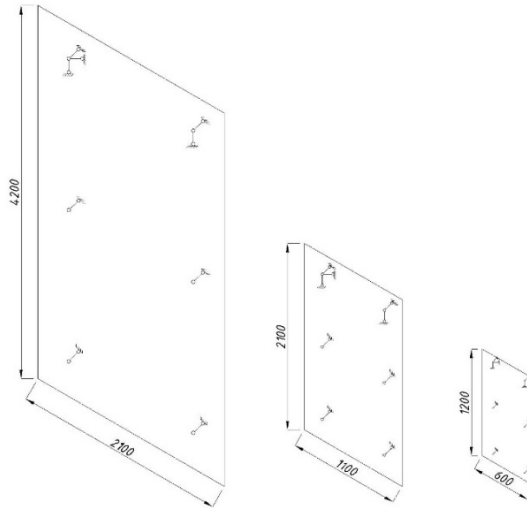

Figure 5. Dimensions of considered panels.

2.3. Applied load

Façade panel was subjected to evenly distributed wind load in accordance with Russian Set of Rules 70.13330.2012 "Load-bearing and separating constructions".

Load value was calculated for the angle zone at the height of +100 m according to Russian Set of Rules 20.13330.2016 "Loads and actions":

$$w_{+(-)} = w_o \cdot k(z_e) \cdot [1 + \xi(z_e)] \cdot c_p \cdot v_{+(-)},$$

where $w_{+(-)}$ is characteristic peak value of positive and negative impact of wind load;

w_o is characteristic value of wind pressure (adopted in accordance with location of construction site):

$$w_o = 0.23 \text{ kPa}$$

z_e is equivalent height ($z_e = 100$ m);

$k(z_e)$, $\zeta(z_e)$ are coefficients, which take into account change of pressure and wind pulsation at the height z_e respectively:

$$k(100) = 2; \quad \xi(100) = 0.54;$$

$v_{+(-)}$ are correlation coefficients which correspond to positive (+) and negative wind pressure (–) in dependence on the area A, which is subjected to wind load; for panel with dimensions $b{\times}h$ = 4200×2100 mm $v_{+(-)} = 0.82$.

c_p is peak value of aerodynamic coefficients of positive (+) and negative wind pressure (–), defined in Russian Set of Rules 20.13330.2016 "Loads and actions":

For façade structures, which are located in angle zone, $c_p = 2.2$. Therefore, formula of characteristic wind load takes the form of:

$$w_{ny} = 0.23 \cdot 2 \cdot [1 + 0.54] \cdot 2.2 \cdot 0.82 = 1.28 \, E.$$

Gerasimova, E.N., Galyamichev, A.V., Mikhaylova, M.K., Dogru, S.

129

Design wind load:

$$w_y = w_{ny} \cdot \gamma_f,$$

where γ_f is safety factor.

$$w_y = 1.28 \cdot 1.4 = 1.79 \text{ kPa}.$$

2.4. Ultimate Limit State

In accordance with Ultimate Limit State requirements, which are defined for toughened glass structures in Russian Set of Rules 20.13330.2016 "Loads and actions", design bending strength value of a glass is equal to:

$$R = 120 \text{ MPa}.$$

2.5. Serviceability Limit State

According to Russian Set of Rules 20.13330.2016 "Loads and actions", deflection of flat glass subjected to the most unfavorable combination of factors should not exceed 1/250 of the shortest side of a panel:

$$|w| = \frac{1}{250} a$$

where a is the shortest side of a panel.

For example, for the panel with dimensions 600×1200 mm:

$$a = 600 \text{ mm};$$

$$|w| = \frac{1}{250} \cdot 600 = 2.4 \text{ mm}.$$

For:

$$a = 1100 \text{ mm} \rightarrow |w| = 4.4 \text{ mm};$$

$$a = 2100 \text{ mm} \rightarrow |w| = 8.4 \text{ mm}.$$

3. Results

3.1. Load distribution

Percentage load distribution in the panels was derived from the internal efforts obtained in software SCAD.

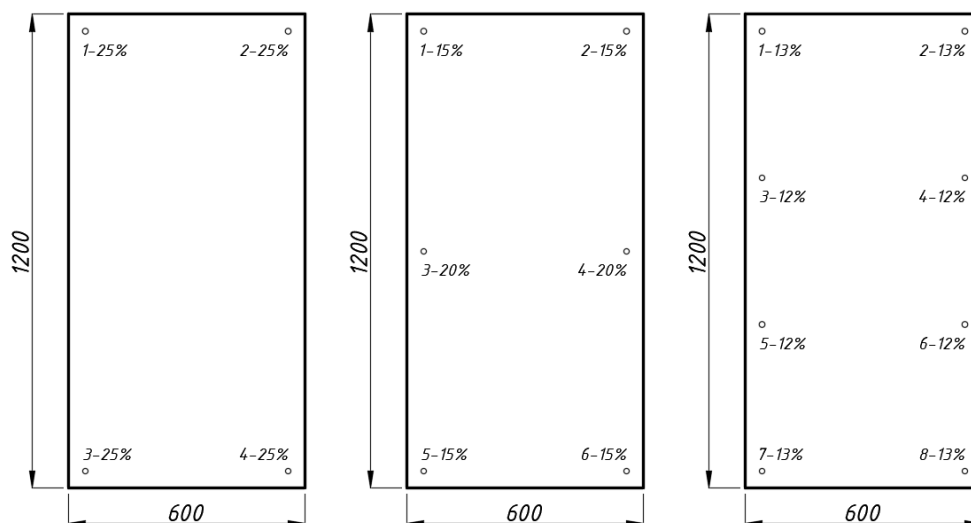Figure 9 presents load distribution to point fixtures from [22].

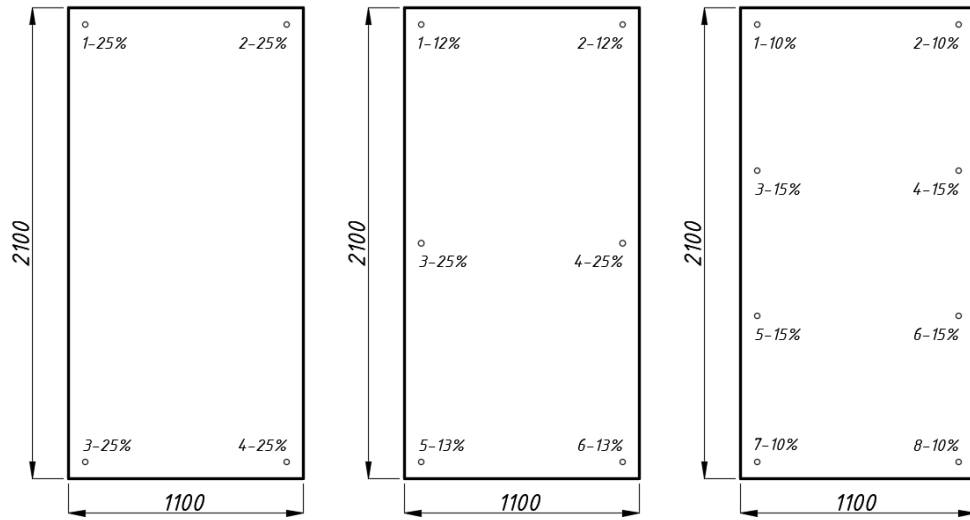**Figure 6. Load distribution to fixtures for the panel 600×1200×10 mm.**

Герасимова Е.Н., Галямичев А.В., Михайлова М.К., Догру С.

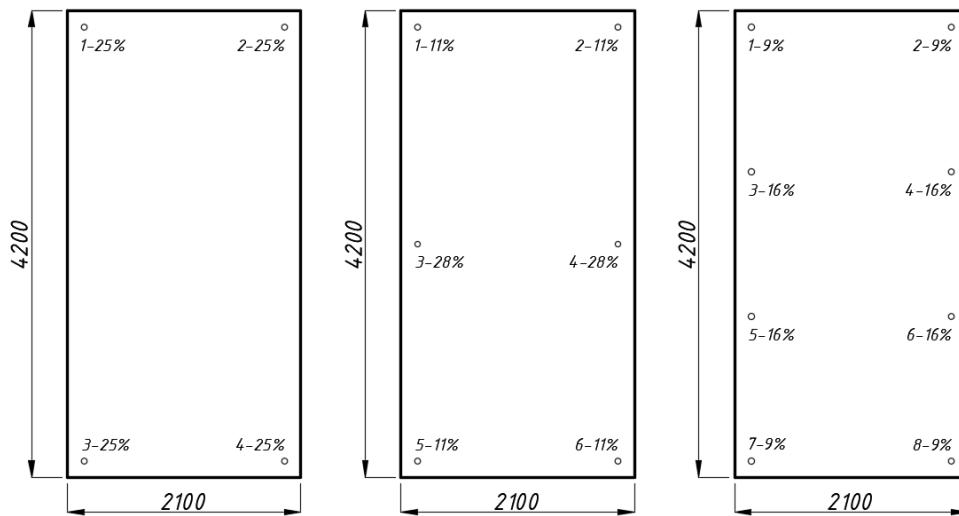**Figure 7. Load distribution to fixtures for the panel 1100×2100×10 mm.**

Figure 8. Load distribution to fixtures for the panel 2100×4200×10 mm.

In the panel with 4 fixtures every point bears 25 % of applied load. In the panels with 6 and 8 fixtures the distribution should be checked as it varies depending on dimensions of the panel.
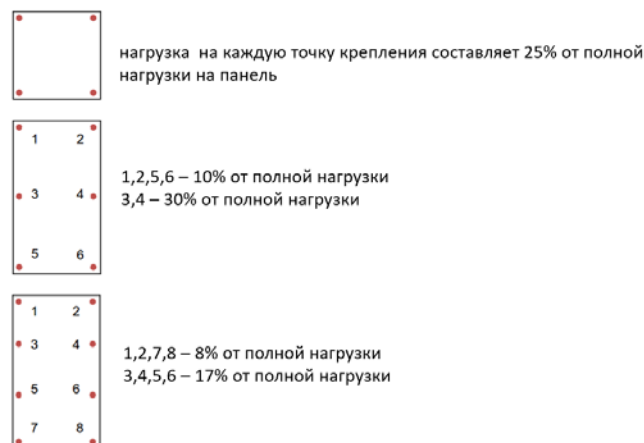

Figure 9. Load distribution to fixtures according to guideline by Dow Corning [22].

Calcilation of inaccuracy between values derived from SCAD and Dow Corning guideline:

$$\delta_{0.6x1.2} = \frac{30-20}{30} \cdot 100 \ \% = 33.3 \ \%;$$

Gerasimova, E.N., Galyamichev, A.V., Mikhaylova, M.K., Dogru, S.

131

$$\delta_{1.1x2.1} = \frac{30-25}{30} \cdot 100 \ \% = 16.7 \ \%;$$

$$\delta_{2.1x4.2} = \frac{30-28}{30} \cdot 100 \ \% = 6.7 \ \%.$$

3.2. Modification of the number of point fixtures

The stresses, which arose in the panels with dimensions $b{\times}h{\times}t$ = 2100×4200×10 mm and different number of fixtures under the action of wind load, are presented below:
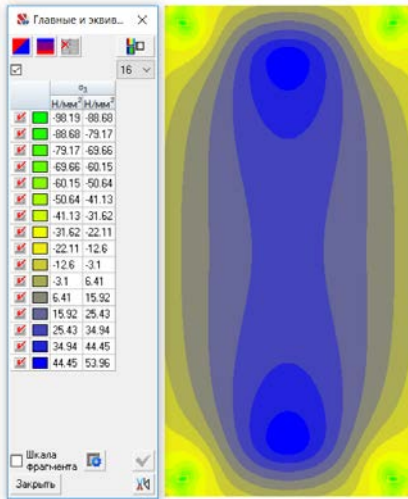

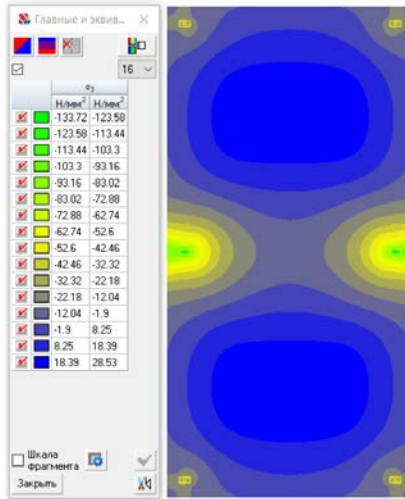**Figure 10. Stresses in panel 2100×4200 mm with 4 point fixtures.**

Figure 11. Stresses in panel 2100×4200 mm with 4 point fixtures.
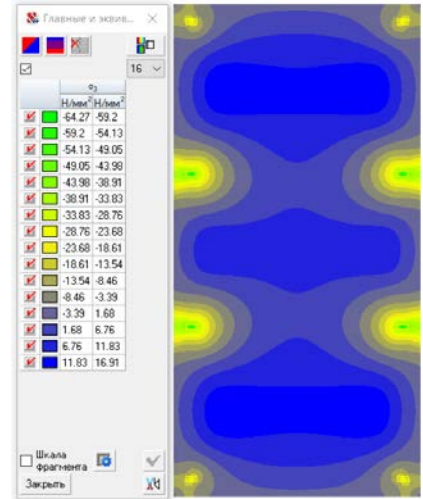
Figure 12. Stresses in panel 2100×4200 mm with 8 point fixtures.

Figure 13 represents graphical dependencies of maximum and average values of stresses on the number of point fixtures.
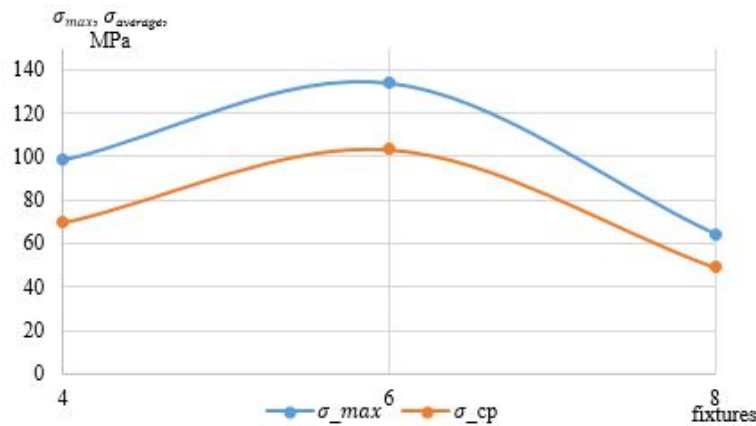

Figure 13. Dependence of maximum and average values of stresses on the number of point fixtures in the panel with dimensions 2100×4200 mm.

3.3. Modification of the thickness of the panel

The deflections in the panels with dimensions $b{\times}h$ = 2100×4200 mm, 6 point fixtures and different values of thickness (t = 8, 10, 12, 14, 16 and 18 mm), are presented below:

Figure 20 represents graphical dependencies of maximum deflections on the value of panel thickness.

3.4. Modification of the value of fixture edge distance

The analysis of influence of edge distance was performed on the panel with dimensions $b{\times}h{\times}t$ = 2100×4200×10 mm while edge distance d was varied for every point fixture.
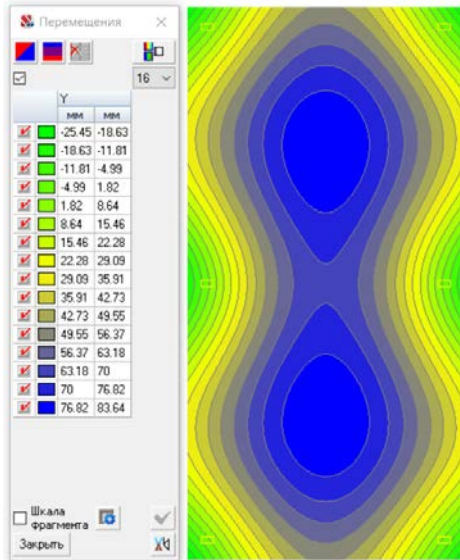
**Figure 14. Deflection in panel
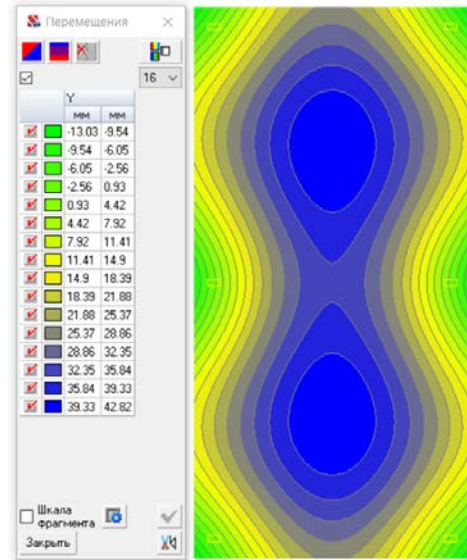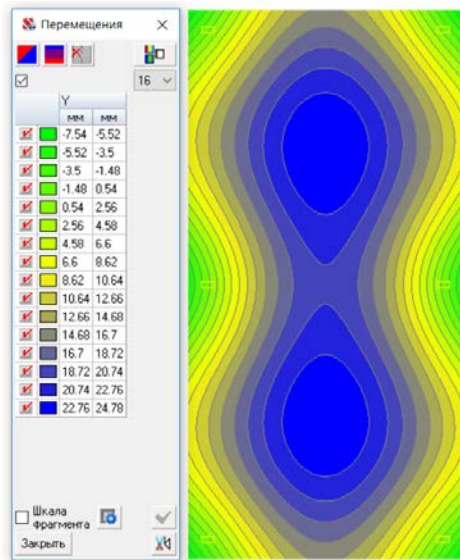2100×4200×8 mm.**

**Figure 15. Deflection in panel
2100×4200×10 mm.**

**Figure 16. Deflection in panel
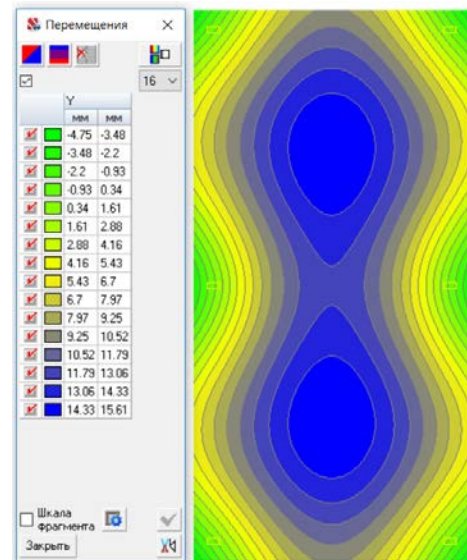2100×4200×12 mm.**

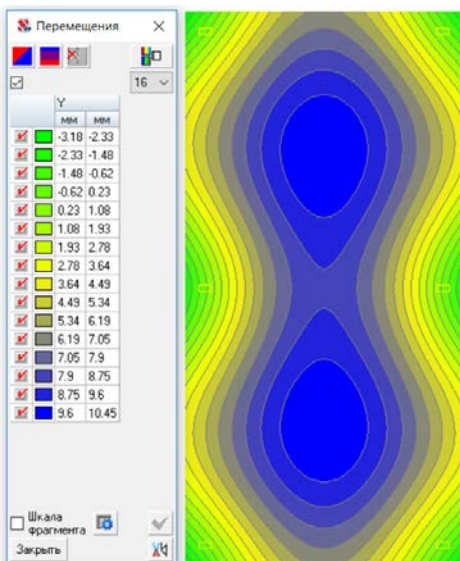**Figure 17. Deflection in panel
2100×4200×14 mm.**
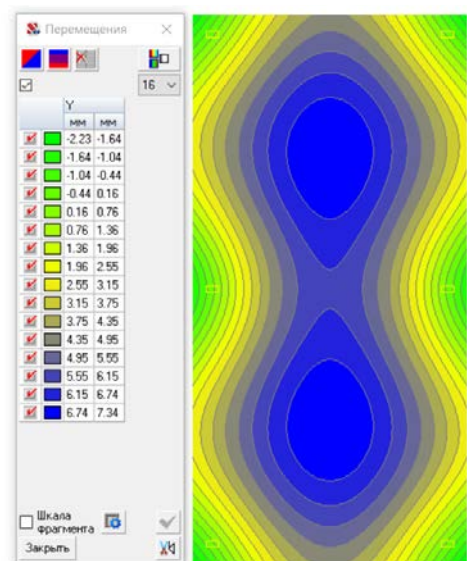

**Figure 18. Deflection in panel
2100×4200×16 mm.**

**Figure 19. Deflection in panel
2100×4200×18 mm.**

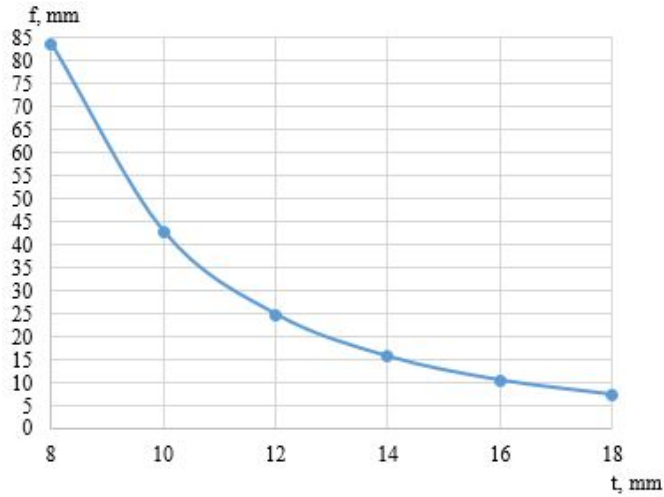Gerasimova, E.N., Galyamichev, A.V., Mikhaylova, M.K., Dogru, S.

133

Figure 20. Dependence of maximum values of deflection on the glass thickness in the panel with dimensions 2100×4200 mm.
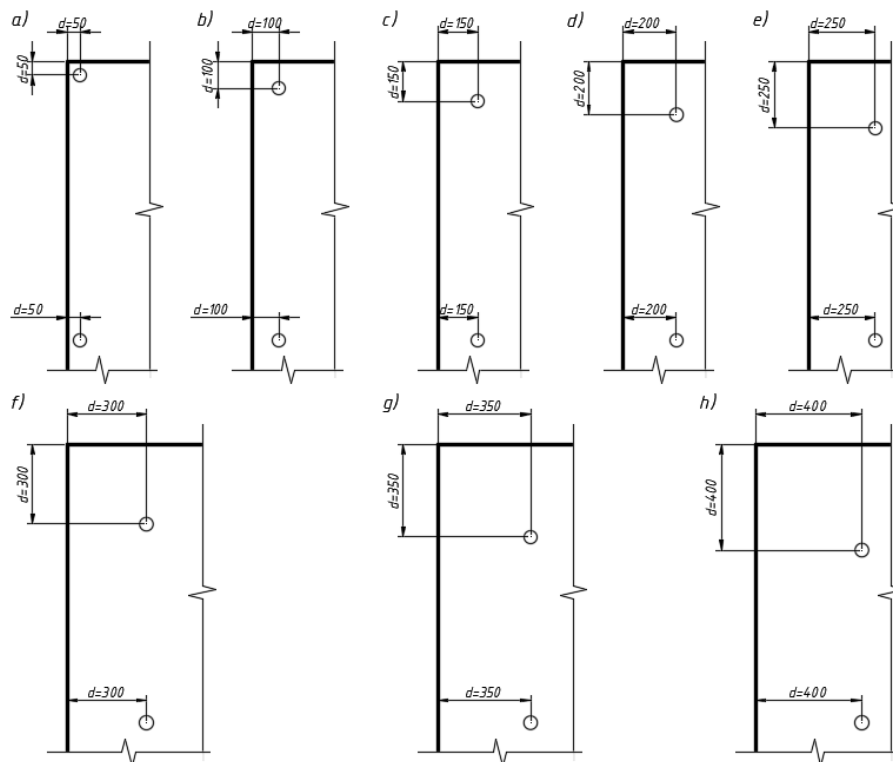

Figure 21. Considered options of point fixture locations relatively panel edge.

As a result, the following diagrams representing stress and deformation distribution in the panels were obtained:

As it can be seen from Figure 38, maximum stresses arose when the edge distance had minimum value. Panels with considered values of edge distance more than 200 mm did not satisfy conditions of Ultimate Limit State.

3.5. Choice of the most optimal structural scheme of façade panel

For the purpose of determination of the most optimal structural scheme, which would satisfy requirements defined by both Ultimate and Serviceability Limit States, a panel with dimensions $b{\times}h{\times}t = 2100{\times}4200{\times}16$ mm, 6 point fixtures and edge distance equal to 200 mm was calculated.
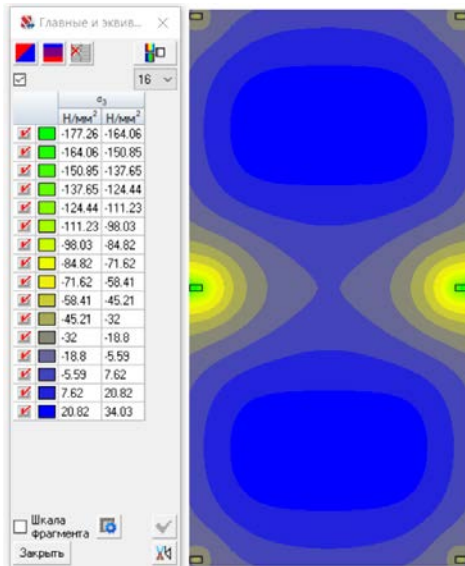
Figure 22. Stresses in the panel with d = 50 mm (a)
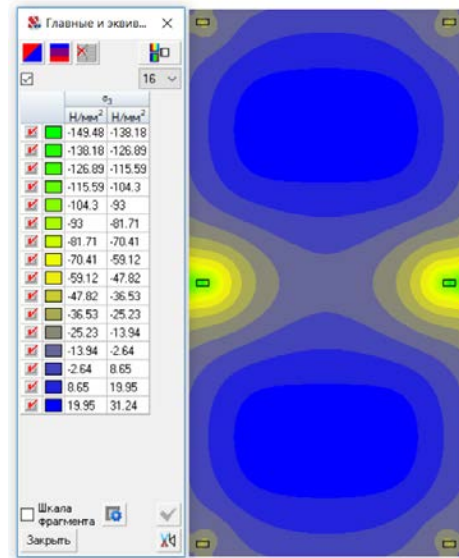

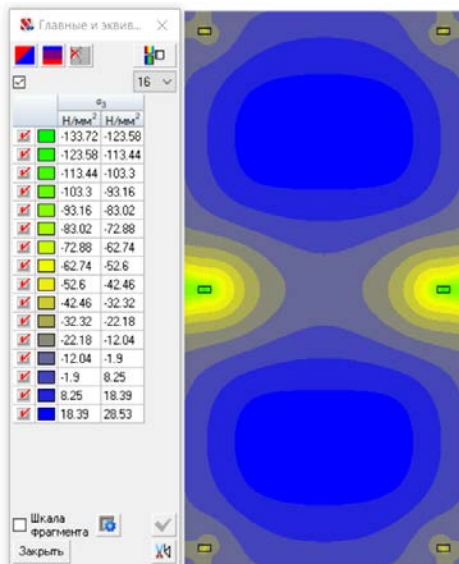**Figure 23. Stresses in the panel with d = 100 mm (b)**

Figure 24. Stresses in the panel with d = 150 mm (c)
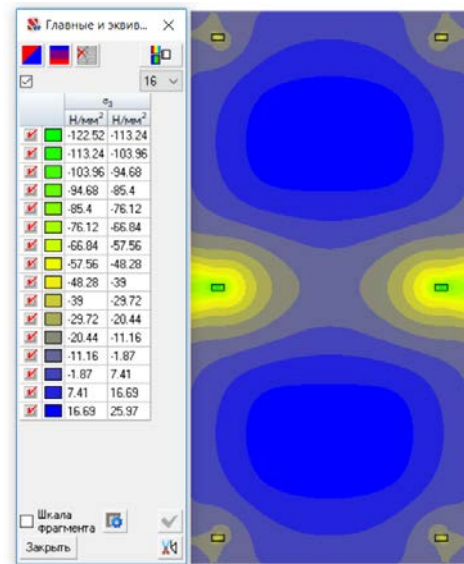

Figure 25. Stresses in the panel with d = 200 mm (d)
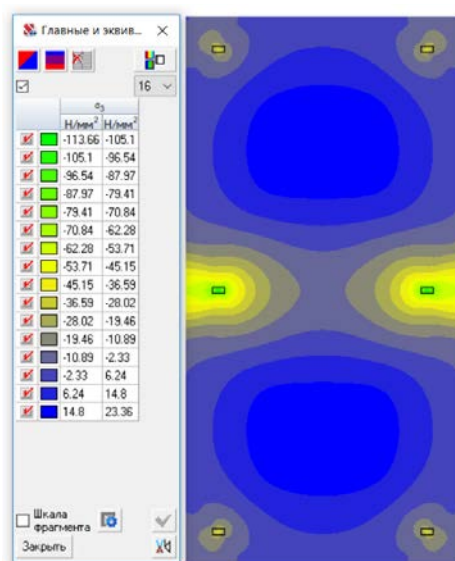
Figure 26. Stresses in the panel with d = 250 mm (e).
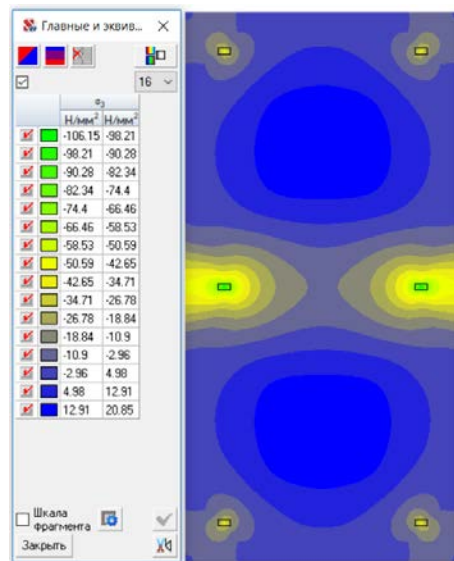
Figure 27. Stresses in the panel with d = 300 mm (f).

Gerasimova, E.N., Galyamichev, A.V., Mikhaylova, M.K., Dogru, S.
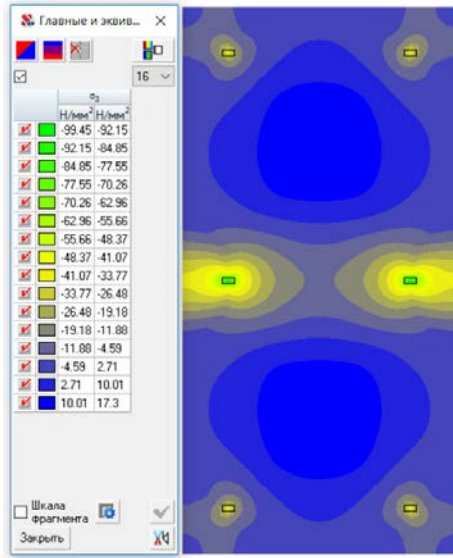
Figure 28. Stresses in the panel with d = 350 mm (g).
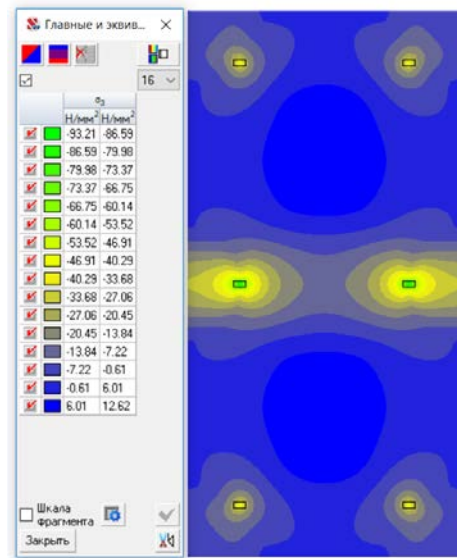
Рисунок 29. Stresses in the panel with d = 400 mm (h).
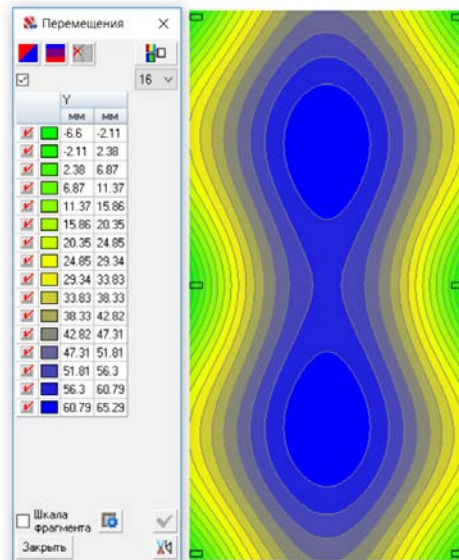
Figure 30. Deformations in the panel with d = 50 mm.
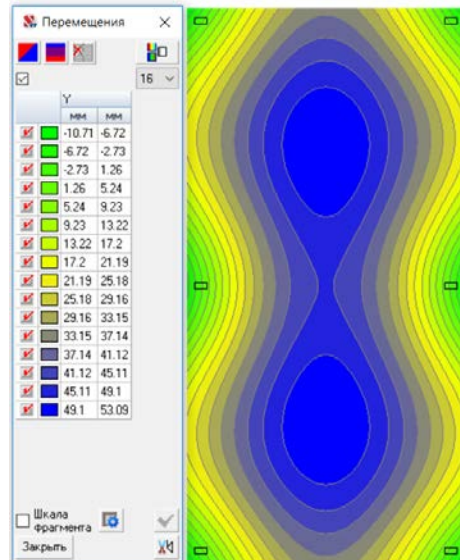
Figure 31. Deformations in the panel with d = 100 mm.
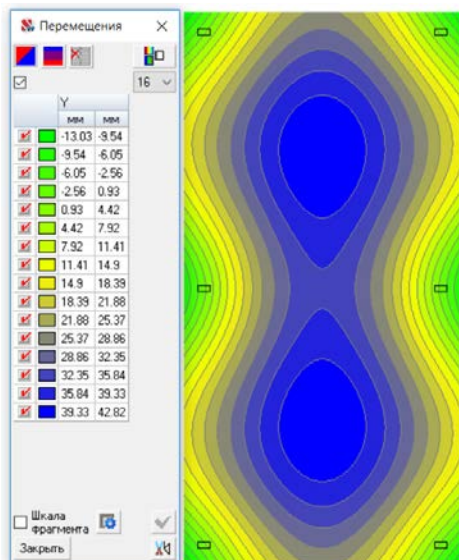
Figure 32. Deformations in the panel with d = 150 mm.
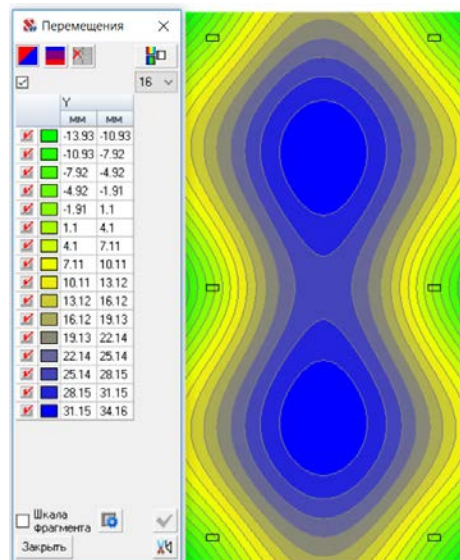
Figure 33. Deformations in the panel with d = 200 mm.

Герасимова Е.Н., Галямичев А.В., Михайлова М.К., Догру С.
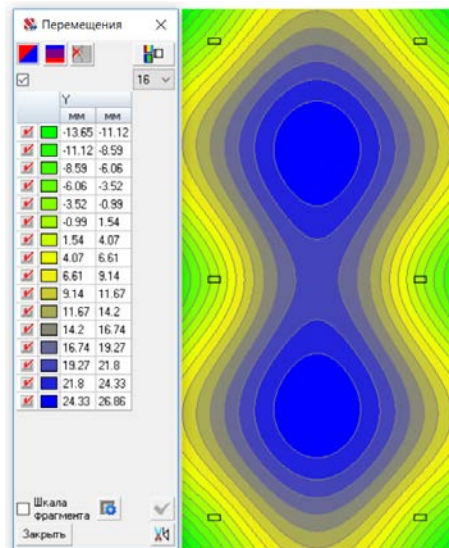
Figure 34. Deformations in the panel with
d **= 250 mm.**
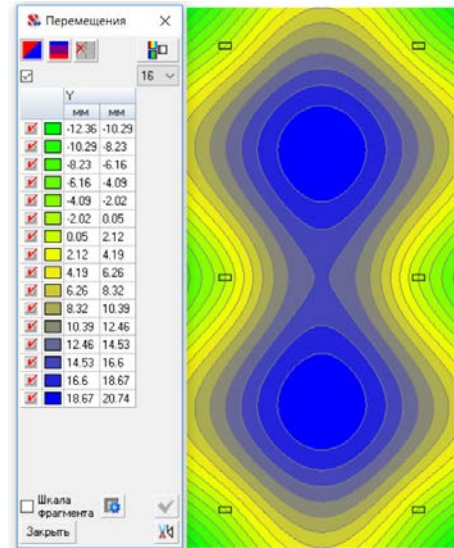
Figure 35. Deformations in the panel
with d **= 300 mm.**
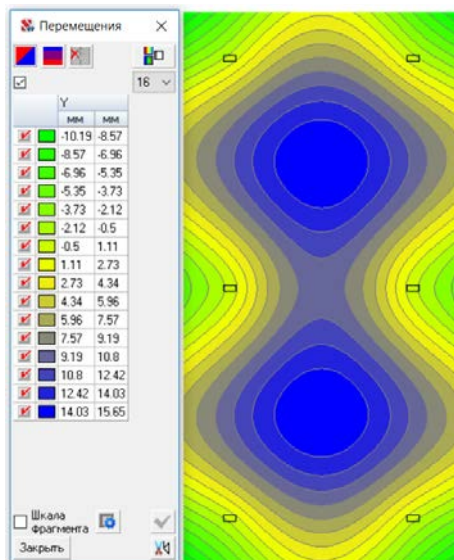
Figure 36. Deformations in the panel
with d **= 350 mm.**

Figure 37. Deformations in the panel
with d **= 400 mm.**
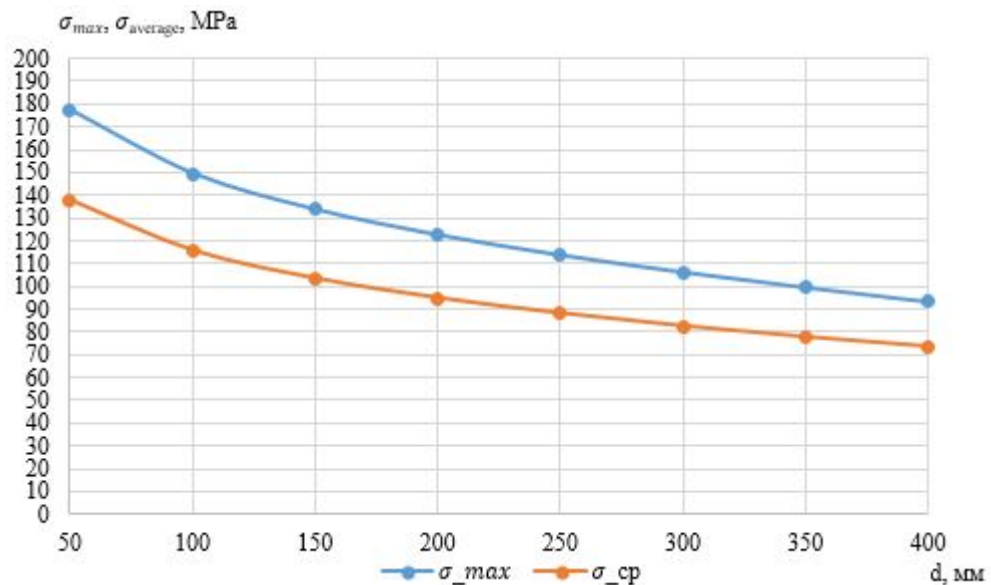
Figure 38. Dependence of maximum and average values of stresses
on the fixture edge distance in the panel with dimensions 2100×4200×10 mm.

Gerasimova, E.N., Galyamichev, A.V., Mikhaylova, M.K., Dogru, S.
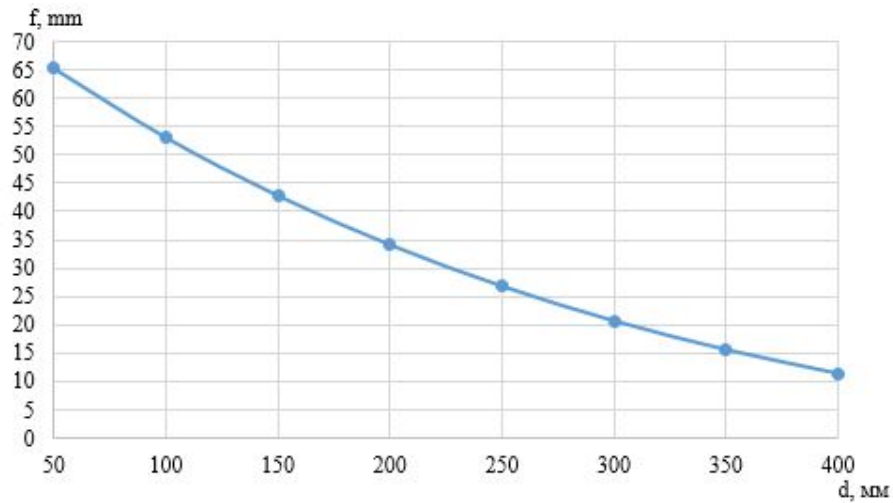
**Figure 39. Dependence of maximum values of deformations
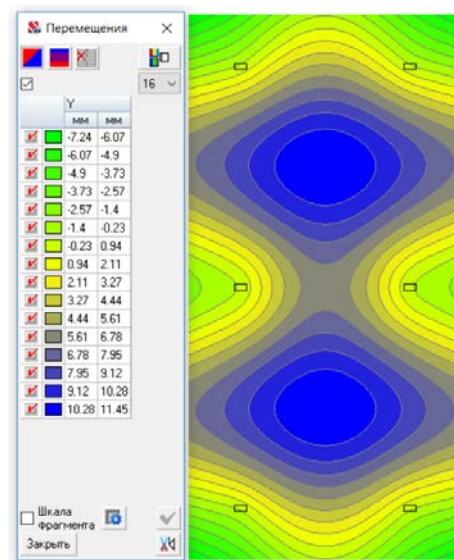on the fixture edge distance in the panel with dimensions 2100×4200×10 mm.**
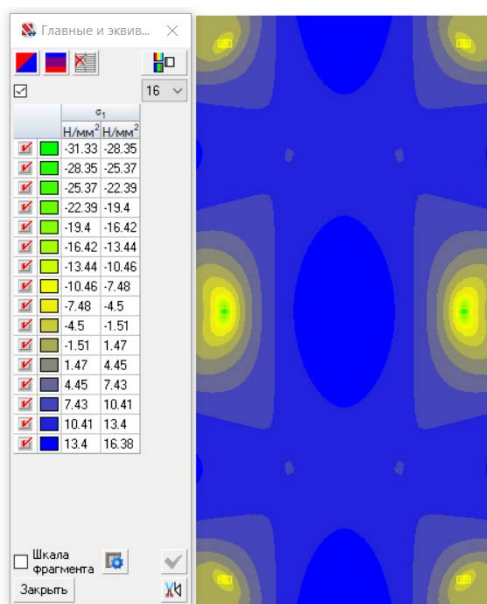
Figure 40. Stress distribution of the panel.   **Figure 41. Deformations of panel.**
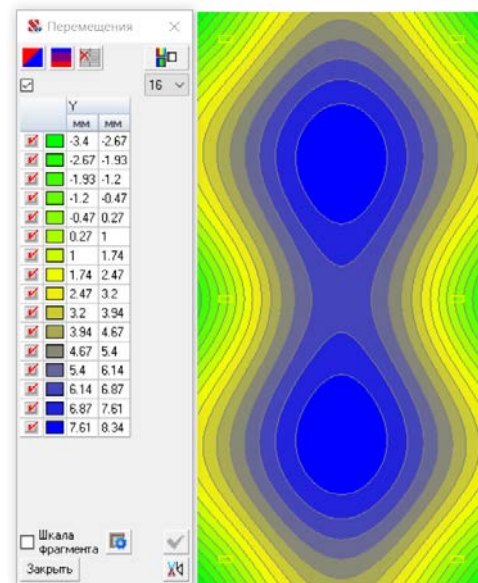
In this scheme the maximum value of the stress which arose on the panel surface σ_{max} equals to 31.35 MPa. This value is significantly smaller, than maximum allowable strength $R = 120$ MPa.

Maximum deflection f_{max} equals to 8.34 mm, what does not exceed maximum allowable value for this panel $|w| = 8.4$ mm.

4. Conclusions

The research purpose of this article consisted in calculation of the façade panels under changing parameters such as number of point fixtures, thickness of a panel, value of fixture edge distance and subsequent analysis of their influence on stress-strain state of the panel.

Based on it, the following conclusions were made:

1. Stresses arising in the panel generally decrease with the number of point fixtures increasing. At same time fixture points are concentrators of the stress, and the maximum stress emerge in center fixtures. However, there are exceptional cases (see 4.2)

2. Increase of the number of fixtures does not always lead to increase of its bearing capacity. It can be illustrated on the example of panel with dimensions $b{\times}h{\times}t$ = 2100×4200×10 mm, which has 6 point fixtures. This panel does not satisfy requirements of ULS, while the same sized panels, but with 4 and 8 fixtures fulfil conditions of Limit State Design. This phenomenon is connected with the fact that in the structural scheme of a continuous beam maximum stress arises in the center support.

Герасимова Е.Н., Галямичев А.В., Михайлова М.К., Догру С.

3. Increase of the panel thickness leads to decrease of deflections of the panel. Maximum deflections appear in the center of the span between fixtures.

4. Increase of the fixture edge distance leads to decrease of both stresses and deflections of the panel. Maximum stresses and deflections arise when the edge distance is minimum. At the same time, if values of edge distance are increased up to 300–400 mm deflections on the edges become comparable to deflections in the center of the span. If edge distances are greater than 400 mm, deflections on the edges exceed deflections in the center of the span.

5. Percentage distribution of the applied load to the fixtures should be calculated for every design case taking into account edge distances and spans between fixtures.

6. Serviceability Limit state is the defining criteria for the design of glass structures in Russian Federation.

References

1. Magay, A.A., Dubynin, N.V. Svetoprozrachnyye fasady vysotnykh mnogofunktsionalnykh zdaniy [Translucent facades of high-rise multifunctional buildings]. Vestnik MGSU. 2010. No. 2. Pp. 14–21. (rus)

2. Patterson, M.R. Structural glass facades: a unique building technology. Master Thesis, University of Southern California. 2008. 450 p.

3. Drass, M., Schneider, J. Constitutive modeling of transparent structural silicone adhesive – TSSA. Proceedings of 14 Darmstädter Kunststofftage – Simulation und Werkstoffmodelle. Darmstadt, 2016.

4. Drass, M., Schneider, J. On the mechanical behavior of transparent structural silicone adhesive – TSSA. Mechanics and Computation. 2016. No. 2. Pp. 20–26. DOI: 10.1201/9781315641645-74

5. Staudt, Y., Schneider, J, Odenbreit, C. Investigation of the material behavior of bonded connections with silicone. Proceedings of International Conference at glasstec. Dusseldorf, 2014. Pp. 10–20.

6. Staudt, Y., Odenbreit, C., Schneider, J. Investigation of Bonded Connections with Silicone under Shear Loading. Proceedings of 4 Conference on Architectural and Structural Applications of Glass. Ghent, 2016. Pp. 3–17.

7. Drass, M., Schneider, J., Kolling, S. Damage effects of adhesives in modern glass façades: a micro-mechanically motivated volumetric damage model for poro-hyperelastic materials. International Journal of Mechanics and Materials in Design. 2017. No. 8. Pp. 20–44.

8. Pascual, C., Montali, J., Overend, M. Adhesively-bonded GFRP-glass sandwich components for structurally efficient glazing applications. Composite Structures. 2017. No. 160. Pp. 560–573.

9. Sitte, S., Brasseur, M.J., Carbary, L.D., Wolf, A.T. Preliminary Evaluation of the Mechanical Properties and Durability of Transparent Structural Silicone Adhesive (TSSA) for Point Fixing in Glazing. Journal of ASTM International. 2011. No. 10. Pp. 4–30.

10. Savitskiy, G.A. Vetrovaya nagruzka na sooruzheniya [Wind load applied to buildings]. Moscow: Stroyizdat, 1972. 111 p. (rus)

11. Cook, N.J. The designer's guide to wind loading of building structures. Part 2: Static structures. London, 1990. 586 s.

12. Nemova, D.V. Navesnyye ventiliruyemyye fasady obzor osnovnyye problem [Ventilated facades: an overview of the main problems]. Magazine of Civil Engineering. 2010. No. 5. Pp. 7–11. DOI: 10.18720/MCE.15.3. (rus)

13. Gorshkov, A.S., Popov, D.Yu. Konstruktivnoye ispolneniye ventiliruyemogo fasada povyshennoy nadezhnosti [Design of the ventilated facade of the increased reliability]. Magazine of Civil Engineering. 2010. No. 8. Pp. 5–9. (rus)

14. Gent, A. Elastic instabilities in rubber. International Journal of Non-Linear Mechanics. 2005. 40(2). Pp. 165–175.

15. Dias, V. Development of adhesives constitutive material laws for the assessment of bonded steel to glass partial composite beams. Doctoral Thesis, University of Luxembourg. 2013. 416 p.

16. Staudt, Y. Investigation of the material behavior of glued connections with silicone. Master Thesis, Technische Universität Darmstadt. 2013.

17. Van Den Bergh, S., Hart, R., Petter, B., Jelle, B.P., Gustavsen, A. Window Spacers and Edge Seals in insulating glass units: a State-of-the-Art Review and Future Perspectives. Energy and Buildings. 2013. No. 58. Pp. 263–280.

18. Wolf, A.T. Silicone Sealed Insulating Glass Units. Proceedings of ISAAG – International symposium on the Application of Architectural Glass. Munich, 2004.

19. Li, X., Li, S., Zia, Q., Zi, H. Effects of pore sizes of porous silica gels on desorption activation energy of water vapor. Applied Thermal Engineering. 2007. No. 27. Pp. 869–876.

20. Baetens, R., Jelle, B.P., Gustavsen, A. Aerogel insulation for building applications: A state-of-the-art review. Energy and Buildings. 2011. No. 43. Pp. 761–769.

21. Dow Corning Official website [Online]. URL: https://consumer.dow.com/en-us.html?_ga=2.83410198.1493760776.1527724064-1652577140.1524781935 (reference date: 02.04.18).

22. DOWSILTM TSSA/TSSL. Techical Manual. 2018.

Contacts:

Ekaterina Gerasimova, +7(921)9673868; katyageras17@gmail.com
Alexander Galyamichev, +7(911)8110719; galyamichev@yandex.ru
Maria Mikhaylova, +7(904)3360888; mmikhaylovaa@gmail.com
Selcuk Dogru, +905305493259; seltrue@hotmail.com

Gerasimova, E.N., Galyamichev, A.V., Mikhaylova, M.K., Dogru, S.

139

Напряженно-деформированное состояние панели из стекла с точечным клеевым креплением

Е.Н. Герасимова[a*], М.К. Михайлова[b], А.В. Галямичев[a], С. Догру[c]
[a] *Санкт-Петербургский политехнический университет Петра Великого, Санкт-Петербург, Россия*
[b] *НИУПЦ «Межрегиональный институт оконных и фасадных конструкций», Санкт-Петербург, Россия*
[c] *İstanbul Okan Üniversitesi, Стамбул, Турция*
* E–mail: katyageras17@gmail.com

Ключевые слова: структурное остекление, силиконовый герметик, точечное крепление, стекло, светопрозрачные конструкции

Аннотация. Статья посвящена исследованию несущей способности конструкции остекления с точечным креплением к несущему основанию. В ней проводится оценка влияния таких факторов, как величина приложенной нагрузки, краевое расстояние, толщина стекла и количество точечных креплений, на напряженно-деформированное состояние панели. Расчет панелей при различных постановках задач проводился методом конечных элементов (МКЭ). Результаты расчета позволяют установить зависимости между рассматриваемыми факторами и напряженно-деформированным состоянием панели, а также определяют возможности использования таких конструкций в соответствии с первой и второй группами предельных состояний.

Литература

1. Магай А.А., Дубынин Н.В. Светопрозрачные фасады высотных многофункциональных зданий // Вестник МГСУ. 2010. № 2. С. 14–21.

2. Patterson M.R. Structural glass facades: a unique building technology. Master Thesis, University of Southern California. 2008. 450 с.

3. Drass M., Schneider J. Constitutive modeling of transparent structural silicone adhesive – TSSA // Proceedings of 14 Darmstädter Kunststofftage – Simulation und Werkstoffmodelle. Darmstadt, 2016.

4. Drass M., Schneider J. On the mechanical behavior of transparent structural silicone adhesive – TSSA // Mechanics and Computation. 2016. No. 2. Pp. 20–26. DOI: 10.1201/9781315641645-74

5. Staudt Y., Schneider J, Odenbreit C. Investigation of the material behavior of bonded connections with silicone // Proceedings of International Conference at glasstec. Dusseldorf, 2014. Pp. 10–20.

6. Staudt Y., Odenbreit C., Schneider J. Investigation of Bonded Connections with Silicone under Shear Loading // Proceedings of 4 Conference on Architectural and Structural Applications of Glass. Ghent, 2016. Pp. 3–17.

7. Drass M., Schneider J., Kolling S. Damage effects of adhesives in modern glass façades: a micro-mechanically motivated volumetric damage model for poro-hyperelastic materials // International Journal of Mechanics and Materials in Design. 2017. No. 8. Pp. 20–44.

8. Pascual C., Montali J., Overend M. Adhesively-bonded GFRP-glass sandwich components for structurally efficient glazing applications // Composite Structures. 2017. No. 160. Pp. 560–573.

9. Sitte S., Brasseur M.J., Carbary L.D., Wolf A.T. Preliminary Evaluation of the Mechanical Properties and Durability of Transparent Structural Silicone Adhesive (TSSA) for Point Fixing in Glazing // Journal of ASTM International. 2011. No. 10. Pp. 4–30.

10. Савицкий Г.А. Ветровая нагрузка на сооружения. М.: Стройиздат, 1972. 111 с.

11. Cook N.J. The designer's guide to wind loading of building structures. Part 2: Static structures. London, 1990. 586 p.

12. Немова Д.В. Навесные вентилируемые фасады обзор основные проблем // Инженерно-строительный журнал. 2010. № 5. С. 7–11. DOI: 10.18720/MCE.15.3.

13. Горшков А.С., Попов Д.Ю. Конструктивное исполнение вентилируемого фасада повышенной надежности // Инженерно-строительный журнал. 2010. № 8. С. 5–9.

14. Gent A. Elastic instabilities in rubber // International Journal of Non-Linear Mechanics. 2005. No. 40(2). Pp. 165–175.

15. Dias V. Development of adhesives constitutive material laws for the assessment of bonded steel to glass partial composite beams. Doctoral Thesis, University of Luxembourg. 2013. 416 p.

16. Staudt Y. Investigation of the material behavior of glued connections with silicone. Master Thesis, Technische Universität Darmstadt. 2013.

17. Van Den Bergh S., Hart R., Petter B., Jelle B.P., Gustavsen A. Window Spacers and Edge Seals in insulating glass units: a State-of-the-Art Review and Future Perspectives // Energy and Buildings. 2013. No. 58. Pp. 263–280.

18. Wolf A.T. Silicone Sealed Insulating Glass Units. Proceedings of ISAAG – International symposium on the Application of Architectural Glass. Munich, 2004.

19. Li X., Li S., Zia Q., Zi H. Effects of pore sizes of porous silica gels on desorption activation energy of water vapor // Applied Thermal Engineering. 2007. No. 27. Pp. 869–876.

20. Baetens R., Jelle B.P., Gustavsen A. Aerogel insulation for building applications: A state-of-the-art review // Energy and Buildings. 2011. No. 43. Pp. 761–769.

21. Dow Corning Official website [Электронный ресурс]. URL: https://consumer.dow.com/en-us.html?_ga=2.83410198. 1493760776.1527724064-1652577140.1524781935 (дата обращения: 02.04.18).

22. DOWSILTM TSSA/TSSL. Techical Manual. 2018.

Контактные данные:

Екатерина Николаевна Герасимова, +7(921)9673868; эл. почта: katyageras17@gmail.com

Александр Викторович Галямичев, +7(911)8110719; эл. почта: galyamichev@yandex.ru

Мария Константиновна Михайлова, +7(904)3360888; эл. почта: mmikhaylovaa@gmail.com

Сельчук Догру, +905305493259; эл. почта: seltrue@hotmail.com

Gerasimova, E.N., Galyamichev, A.V., Mikhaylova, M.K., Dogru, S.

141